

## Inkjet Printing of Thick-Film Resistors

Marcel Wassmer, Waldemar Diel, Klaus Krueger

Institute of Automation Technology, Helmut-Schmidt-University / University of the German Armed Forces,  
Holstenhofweg 85, 22043 Hamburg, Germany

Marcel Wassmer: Phone +49/(0)40/6541-2324, Fax +49/(0)40/6541-2004, E-Mail: marcel.wassmer@hsu-hh.de

Waldemar Diel: Phone +49/(0)40/6541-3805, Fax +49/(0)40/6541-2004, E-Mail: diel@hsu-hh.de

Klaus Krueger: Phone +49/(0)40/6541-2722, Fax +49/(0)40/6541-2004, E-Mail: klaus.krueger@hsu-hh.de

### Abstract

*The integration of passive components directly into circuit board is an efficient alternative to surface mounted devices. Inkjet printing is the emerging technology for the deposition of a variety of particles and therefore for digital fabrication of microelectronic circuits. Resistors are one of the most frequently required passive components in electronic circuits. In LTCC-technology the integration and additionally the embedding of resistors promises new applications. Integrated resistors are usually screen printed. Inkjet printing has several advantages to compete seriously with screen printing as production method. This study investigates the possibilities and reliability of inkjet printing of thick-film resistors.*

*In a first step, different resistive compositions are characterised towards compatibility with a commercial inkjet print head. The reliability and long term stability in drop formation are fundamental for production process. Further on, the interaction between ink and substrate has to be taken into account to reach the desired morphology.*

*In a second step, the advantages of using inkjet for printing resistors are shown. A measure of ink amount is introduced for exact dosing of the ink. Afterwards, compositions with a wide resistivity range are printed with different print heads. The printed resistors are further passed alternatively through a post-fire or through a co-fire process. The effect of variations in particle composition and ink amount are characterized towards the change in electrical behaviour. Further, the influences of printing conditions on morphology and resistivity are discussed.*

*Key words: inkjet, resistor, thick-film, ink amount, LTCC*

### Introduction

Inkjet printing allows fast digital processing of image data without any kind of mask. It is a flexible and material saving technology for digital fabrication which avoids contact to the substrate and previously printed layers. When using particle inks with electrically functional particles, it has the capability for the fabrication of thick-film components for microelectronic circuits.

Conductive silver lines are the basis for such circuits and might consist of nano-silver particles [1] [2]. As the most important influences on particle ink composition and stability are known quite well [3], inkjet printing becomes more reliable and thus applicable for thick-film printing. To compete with screen-printing next step of investigation necessarily has to be the realization of passive electronic components by ink-jet printing.

The realization of capacitors is complicated, as several different functional layers have to be printed on top of each other. In common screen printing process each layer passes through a printing, drying and sintering step. At least four passes are necessary. Finally, there are strong irregularities in thickness and the variance in capacity is about  $\pm 25\%$  [4]. New high- $k$  particle compositions for thick-film screen printing promise high capacitances and compatibility with low-temperature co-fired ceramic (LTCC) substrates [5]. This is achieved by inorganic additives and particle size reduction [6]. Whereas smaller particles are a challenge for conventional screen printing, they are positive on the requirements for inkjet printing. The reliability of inkjet printed thick-film capacitors is proven in plate design [7] and interdigital design with several dielectric materials [8].

Thick-film printing of inductors is not so common, even though it is in principle very similar to conductor line printing. Inductors gain in importance

for high-frequency and filter applications [9]. The processing of the required ferrite material can hardly be achieved by screen printing. New ferrite particle compositions [10] for LTCC tape production with high permittivity up to 800 promise the integration of inductive components as embedded elements with an elevated inductance [11]. Inkjet printing of ferrite layers is more flexible towards circuit design, further on it promises material saving. The reliability of inkjet printed thick-film inductors is proven in flat square coil design with several ferrite core materials [12].

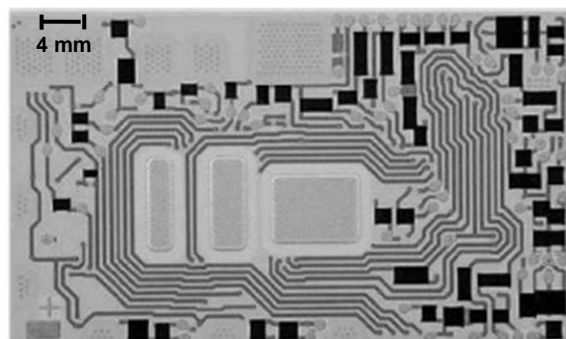


**Figure 1** Thick-film resistors (black areas) on the back side of a micro hybrid circuit

Considering the existing knowledge of inkjet-printed conductor lines, inductors and capacitors [2] [7], it is consequential to investigate the realization of resistors. Thick-film resistors (TFR) are widely used in electronic circuits. They serve as voltage or current divider or in filters with other passive components. Frequently, they are applied as termination, pull-down or pull-up resistor. They can also be implemented as sensors for strain, temperature and pressure or as heaters [13] [14] [15]. The production tolerance of the resistance value is about  $\pm 40\%$  [16].

About 50 % of thick-film resistors used in micro hybrid circuits are in the range up to 1 k $\Omega$ , less than 3 % are higher than 100 k $\Omega$  [17]. When possible the resistors are embedded in multi layer circuits but usually they are placed on the backside. In **figure 1** TFR on the backside of a micro hybrid circuit are shown. To reduce their variance of 40 % to less than 5 % laser trimming can be applied. Although, the fundamental construction rules of inkjet printed TFR do not differ from screen printing, the deposition and behavior of the inks differs significantly from that of pastes, thus an adaptation of the whole printing process is required.

## Experimental Approach

### Ink Preparation

The used resistor inks (RI) are a precise composition of different organic and inorganic ingredients.

Organic ingredients are the composition of solvents and several binders and surfactants. The particle composition is inorganic. The main components are the electrically conducting ruthenium dioxide and different isolating borosilicate glasses to adjust the resistivity. Besides these, several additives (metals and metal-oxides) are used to adjust the thermal coefficient of resistance (TCR) and the thermal coefficient of expansion (TCE). The mean diameter of the particles varies from 60 nm to 1  $\mu\text{m}$ . The inks cover a range of five resistance decades ( $R_{sq}$ ). Following the index of the RI expresses the exponent of the resistance decade.

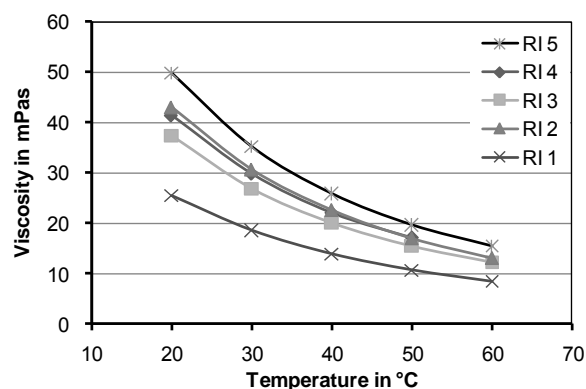


**Figure 2** Shear viscosity of the used resistor inks with different decades of resistance

The preparation of a suitable ink is based on two essential steps. Initially a paste with high solid substance content is prepared. Afterwards, the paste is diluted to an ink with a viscosity suitable for inkjet printing. The RI are all based on the same composition of solvents with a solid substance amount (SSA) of 30 wt.-%. **Figure 2** shows the viscosity of all the used RI. The viscosity depends strongly on temperature. By trend, an increase in viscosity can be observed with increasing resistance decade of the ink. This is caused by an increasing fraction of glass particles with low density, which leads to an increasing volume fraction of solid substance in the ink. Nevertheless, at 40 °C all inks are printable with a commercial inkjet printer. The ink formulations are further tested for stability and reliability in a printing system.

### Printing Equipment

All resistor inks are printed with a self engineered printing system. The print head is a commercial Microdrop MD-K-140 mono dispenser with a nozzle diameter of 50  $\mu\text{m}$ . It is fixed on a carrier, while the substrate is moved underneath by a planar motor. The system is equipped with a nozzle surveillance camera and stroboscopic LED to investigate the stability of the drop formation. The ink meets the requirements, when it shows a long-term stable drop formation and

when it doesn't leave too many residues of particles after first flushing and cleaning of the head. In our case, the drop volume of a stable drop varies for the different RI between 120 and 150 pL.

A second camera system is used for exact positioning of the print head towards the substrate. The substrate can be heated up to 120 °C by a heating plate mounted on the motor's stator.

#### Resistor Printing and Processing

To evaluate resistor printing for co-firing and post-firing process the RI are printed both, on unfired LTCC tapes and on fired LTCC substrates. Both kinds of substrates (1×1 inch<sup>2</sup>) carry an identical silver conductor pattern, which allows for printing eleven rectangular resistors of length  $l_R = 2$  mm and width  $b_R = 1$  mm. The overlap on termination is set to 300 μm. The resistors are built up using inkjet printing with different drop pitches and different numbers of applied layers. The ink amount and consequently the thickness of the resistors  $h_R$  is varied. During printing the temperature of the substrates is set to 70 °C. After drying the resistors are post-fired at 900 °C for 30 min or accordingly laminated and co-fired at the same temperature profile.

#### Ink amount

One advantage of inkjet printing is the capability of very exact dosing in the range of ± 2 %. Whereas screen printing applies all the paste in one pass, inkjet process applies a large number of small drops. This leads to the possibility to control the resistance value of each resistor individually by applying a specific amount of ink. Assuming, a rectangular resistor consists of  $k$  individual layers. Each layer is printed with  $N^L$  overlapping lines in the distance  $\Delta y$  consisting of  $N^D$  overlapping drops in the distance  $\Delta x$ . The applied area load

$$\rho = \frac{\sum_{i=1}^k \cdot N_i^L \cdot N_i^D \cdot m_{D,i}}{A_R} \quad (1)$$

represents the mass of the ink per finally covered area  $A_R$  (further labelled: specific ink amount). The mass of the individual drop  $m_D$  can be determined in several ways. First method uses the nozzle surveillance camera to record the drop contour. The drop radius  $R_0$  can be evaluated by image processing. It is possible to calculate the drop mass

$$m_D = \frac{V_0}{\rho_D} \quad (2)$$

using the relation

$$V_0 = \frac{4}{3} \pi \cdot R_0^3 \quad (3)$$

for the drop volume  $V_0$  and the density  $\rho_D$  of the ink.

The second method uses the spot contour of the placed drop. It is recorded by the positioning camera and the spot radius  $R_S$  can also be evaluated by image processing. The drop mass is then calculated by equation (2) using

$$V_0 = R_S^3 \cdot \pi \cdot \frac{(1 - \cos \theta)^2 \cdot (2 + \cos \theta)}{3 \cdot \sin^3 \theta} \quad (4)$$

as the drop volume, with  $\theta$  representing the contact angle of the ink on the substrate.

The last method uses a large number of drops  $N$  (>10000) that are placed under printing conditions into a container. The container is weighed before and after printing on a high precision balance. The mean drop mass

$$m_D = \frac{\Delta m}{N} \quad (5)$$

is averaged from the mass difference  $\Delta m$ .

All measurements show an accuracy of 5 % or less. As weighting is the simplest method, it is used for these experiments. To avoid random error the measurement is passed twice and repeated frequently.

#### Construction and Calculation

The resistance value of a usual conductor can be calculated by

$$R = \rho_R \cdot \frac{l_R}{A_R} \quad (6)$$

with the specific resistance  $\rho_R$  of the material, its length  $l_R$  and cross section area  $A_R$ .

Industrial pastes for TFR screen printing are available in a large range of 10 to 10<sup>7</sup> Ohm. The choice of material depends on reproducibility and long term stability. Additional requirements are a low TCR, low noise and good trimming characteristics. Resistor pastes are normally offered in a system of different resistance decades. This is achieved by changes in the composition of the paste, resulting in a different specific resistance.

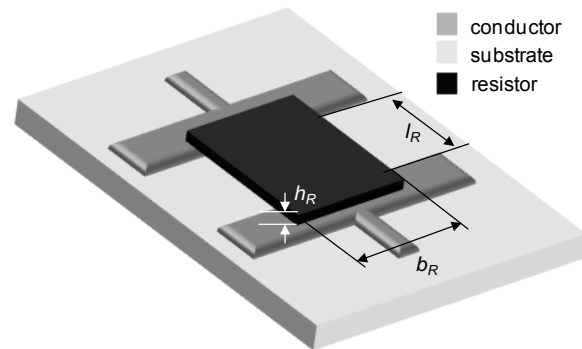


**Figure 3** Rectangular TFR on termination with geometric aspects

The easiest design to realize TFR is the rectangular shape. Its geometric aspects are shown in **figure 3**. Other designs as meander and hat resistors are rarely used and therefore not further considered [15][17][18]. The resistance value

$$R = R_{sq} \frac{l_R}{b_R} \quad (7)$$

of a rectangular TFR depends, besides on the square resistance  $R_{sq}$ , on the aspect ratio of its length  $l_R$  to its width  $b_R$ . The change in aspect ratio is the common way to adjust the resulting resistance value of a screen printed resistor. Typical minimum length and width are 0.5 mm. Good results are achieved with an aspect ratio of 2:1 [4]. The square resistance

$$R_{sq} = \frac{\rho_R}{h_R} \quad (8)$$

results from the specific resistance  $\rho_R$  and the resistor height  $h_R$ . This relation is simplified. The specific resistance is not really constant within the resistor, as diffusion processes take place in the boundary area. Its mean value slightly depends on aspect ratio, material composition and surrounding material [19]. The knowledge of the influences on the resistance value is important, when evaluating the inkjet process for the fabrication of TFR. The conduction mechanism in TFR is well investigated but not completely understood [18][20][21]. The main factor for conductivity is the fraction of ruthenium dioxide particles on overall solid substance volume and the type of glass particles. There is also a big influence of the particle size of both  $\text{RuO}_2$  and glass [22]. Another significant influence on resistance value is given by the parameters of the sintering process. The softening of the glass does not just influence the adhesion of the TFR. In fact, it influences the development of the resistance value during sintering. Most significant parameter is the maximum temperature in addition with its dwell time [23][24]. Differences in the resistance value can further be caused by interaction with the substrate [25], cover layers [26] and surrounding LTCC-layers [19]. As these interactions are boundary effects, the thickness of the resistor plays an important role [27] as well as the composition of the interacting materials [28].

### Geometrical and Electrical Results

The geometrical properties of the printed structures are measured after drying and firing using a light microscope with a measurement unit as well as a white light interferometer. The electrical properties are analyzed with a high precision LCR meter.

**Figure 4** shows the uniformity of the resistor edges. The different occurrence of the resistors' surface in reflected light is expected, due to

their different composition. The surface of the resistors is not exactly rectangular and slightly wavy, due to the large applied amount of solvent. This can be reduced with improved drying of the printed layers. Due to slight differences in physical properties the spreading of the higher RI decodes is marginally lower. This is taken into account when the printing pattern is planned. Finally, the mean deviation of the base area ( $2.6 \times 1.0 \text{ mm}^2$ ) is less than 4 %.

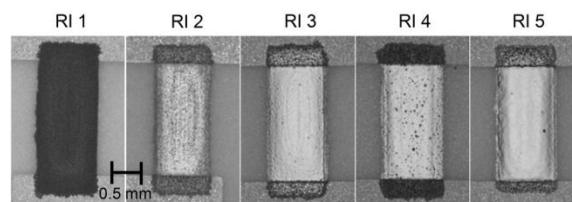


**Figure 4** Surface of the inkjet printed TFR on LTCC after post-firing

The different roughness and waviness of the surface after firing can be measured with the white light interferometer. **Figure 5** shows the surface of RI 5 (top) and RI 1 (bottom). The higher glass amount in RI 5 leads to a smooth surface after firing. Additionally, from this surface data the medium height of the resistors can be calculated.

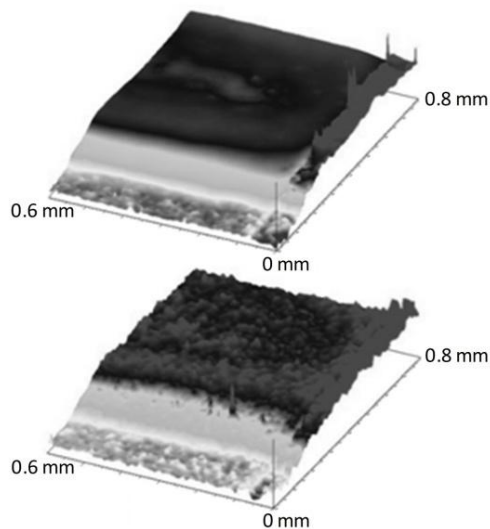


**Figure 5** Surface measurement of TFR: RI 5 (top) and RI 1 (bottom); height is ten times super-elevated

**Figure 6** shows the thickness measurement of RI 1. The measurement shows a strong variance. Nevertheless it can be seen, that the height of the fired resistor is larger than calculated by

$$h_R = \frac{V_{SSA}}{A_R} = \frac{SSA \cdot \rho}{\rho_{SSA, RI}} \quad (9)$$

with the SSA, that is 0.3 for all inks and the individual density of the solid substance, which is for

example  $4.7 \text{ g}\cdot\text{cm}^{-3}$  for RI 1. The difference in resistor height of about +20 % indicates strong migration of glass from substrate into the resistor as well as a certain porosity.

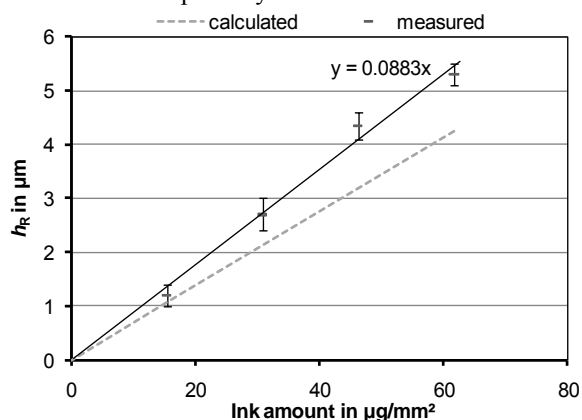


**Figure 6** Resistor height in relation to applied ink amount (RI 1)

For all other RI the variance of the height measurement remains high. Nevertheless, its mean value fits the calculated height with deviation < 5 %. Therefore, minor migration effects and porosity are assumed. Concluding from the applied height measurements, this method seems not an appropriate technique to approximate the resistance value, as several measurements are required. Even more, as it is not possible during printing.

For first experiments the ink amount is varied on each substrate in a small range and with small steps.

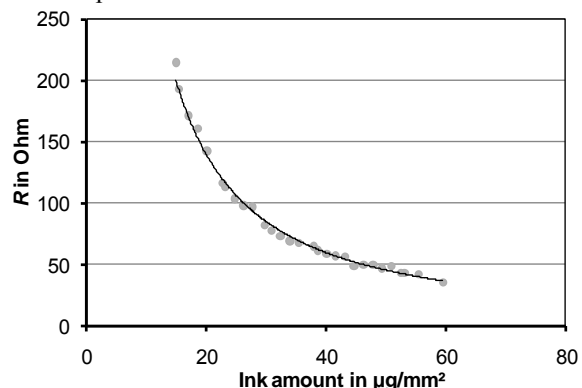


**Figure 7** Resistance value of post fired resistors depending on applied RI 1

**Figure 7** shows the resulting resistance values achieved with varying amount of RI 1 after printing and drying on fired LTCC and post-firing. Note that each spot is just a single resistor. The resistance value of RI 1 is approximated to

$$R = 5400 \text{ Ohm} \cdot \left( \frac{\rho}{\mu\text{g}\cdot\text{mm}^{-2}} \right)^{-1.2} \quad (10)$$

with regression analysis (power function).

The slope of the power function is close to the theoretical value of -1, which was expected from the exponent of  $h_R$  in equation (8). Altogether, the thickness of the resistors is very low, what might increase the influence of diffusion and cause the higher slope. This trial is repeated with RI 4 showing similar behavior. With the other RI the printing scheme is slightly changed. The resistors on a substrate are printed with the same specific ink amount to reveal the standard deviation  $\sigma$  of the resistance value.

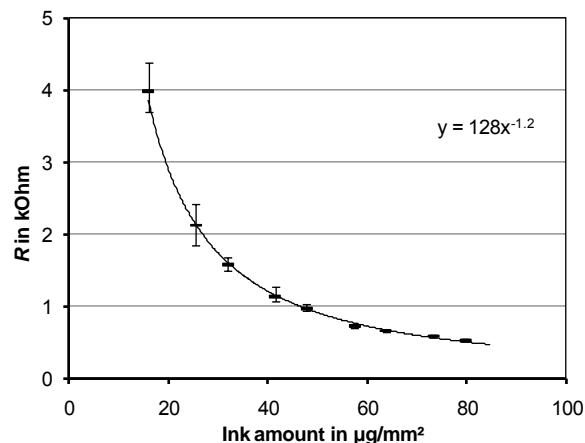


**Figure 8** Range of resistance values of RI 3 and range from minimum to maximum value on a substrate with same ink amount

**Figure 8** shows the maximum and minimum value on the individual substrates for RI 3. The deviation increases with decreasing ink amount. At high ink amount the standard deviation is about 2 % and rises to 7 % at low ink amount. This behavior can be observed for all inks, additionally the overall standard deviation increases at higher decades.

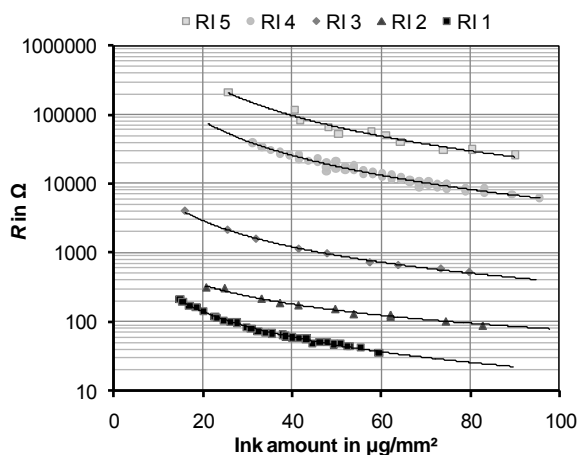


**Figure 9** Range of resistance values of post fired resistors depending on applied RI and ink amount

**Figure 9** shows the summarized results of all post-fired resistors. All decades reveal the same expected behavior. To keep track, the individual slope of the resistor decades is listed in **table 1**. RI 2 shows the expected exponent of -1 and at higher decade the exponent becomes larger, which means equation (8) has to be adapted to each ink.

**Table 1:** Regression results (power function) for resistance value fitting curve and standard deviation (post-firing)

RI	Base in $\Omega$	Exponent	$\sigma$
1	$5.4 \cdot 10^3$	-1.2	-
2	$7.2 \cdot 10^3$	-1.0	< 5 %
3	$128 \cdot 10^3$	-1.2	< 7 %
4	$10 \cdot 10^6$	-1.6	-
5	$50 \cdot 10^6$	-1.7	< 8 %

In common, the resistor ink decades are not balanced exactly. The increment in resistance value between

the decades varies between factor 4 and 20 instead of regular factor 10. The spots of RI 2, 3 and 5 symbolize the mean resistance value of eleven identically printed resistors on a substrate. The standard deviation  $\sigma$  is 7 % or less and depends strongly on the applied ink amount. Following the previous results that show an increased slope of the fitting curves, this is not amazing. On the one hand, this indicates again a relatively stronger interaction of the thin resistors with the substrate and termination. On the other hand, the exact dosing of inkjet printing is proven with this good reproducibility of resistance value.

In parallel, the resistor inks were inkjet printed on LTCC tape and passed through co-fire process. It is not surprising that the basic behavior of the resistor inks does not differ much from previous results. There are two main differences in co-fire process. First, the resistors are laminated with the substrates and second, they are fired between two layers of dielectric, which might increase boundary effects.

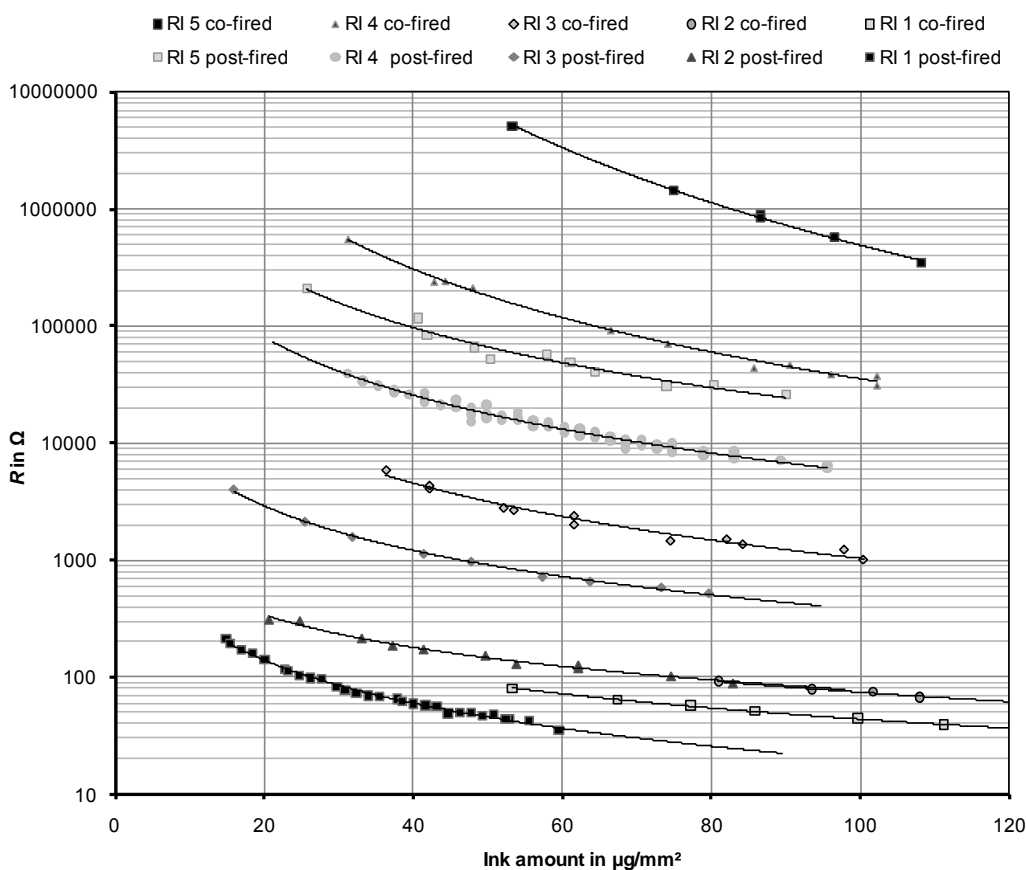


**Figure 10** Range of resistance values depending on ink amount for all resistor inks (RI); summary and comparison of the results of post-fire and co-fire process

The results of all inks are shown in **figure 10**, compared with post-fire results. The comparison reveals that co-firing causes a strong increase in resistance value at all decades, except RI 2. This is observed especially for RI 5 and also RI 4, that is even higher than RI 5 after the post-firing process. These compositions have a low fraction of RuO<sub>2</sub> and are therefore very sensitive to interaction with the substrate. This interaction is enforced in co-fire process. RI 2 seems to be very stable versus migration and boundary effects. Regarding RI 1, also an interaction with the substrate can be assumed.

Additionally, an even stronger increase in slope of the fitting curve is observed at the high decades. The results of the power function regression are listed in **table 2**. At RI 4 and RI 5 the exponent reaches -2.4 and -3.8 respectively. In these cases the resistance value is extraordinary sensitive. Nevertheless, the exact dosing of inkjet printing allows reproducible and individual resistance values. Although, the inks are very sensitive the standard deviation on a substrate is lower than 20 %.

**Table 2:** Regression results (power function) for resistance value fitting curve and standard deviation (co-firing)

RI	Base	Exponent	$\sigma$
1	$3.9 \cdot 10^3$	-1	< 5 %
2	$5.3 \cdot 10^3$	-1	< 4 %
3	$2 \cdot 10^6$	-1.6	< 7 %
4	$2 \cdot 10^9$	-2.4	< 12 %
5	$2 \cdot 10^{13}$	-3.8	< 20 %

## Conclusion

Thick-film resistors can be printed successfully and long term stably with an inkjet printer. Different resistor ink compositions with 30 wt% solid substance, covering a wide range of resistance values, are compatible with the print head. The self-engineered printing system is optimized for resistor printing. It is shown that the controlled deposition of the ink on the substrate leads to regular geometrical properties. The fine and exactly dosing of the print head allows to control the applied ink mass per area (ink amount). The resistance value correlates directly with this applied ink amount. The variation in ink amount could be capable of reducing or replacing the trim process in some cases. A low standard deviation is achieved in the range of  $\sigma < 4$  %, depending on ink and processing. The used inks are suitable for post- and co-fire process, but need further calibration to the used substrate and

process. The shown experimental setup could easily be used for ink calibration and test purposes.

It is demonstrated that inkjet technology has the capability to build-up thick-film resistors at least as accurate as screen printing and gives new opportunities for the design and built-up.

## References

- [1] Albertsen A. et al.: "Combined Manufacture Method for High Density LTCC-substrates: Thick Film Screen-printing, Ink-jet, Post-firing Thin-film Processes and Laser-drilled Fine-vias". Proceedings 4<sup>th</sup> Internat. Conference on CICMT, Munich, Germany, April, pp. 604-610, 2008
- [2] Cibis D.; Krueger K.: "DoD-printing of conductive silver tracks". Proceedings 1<sup>st</sup> Internat. Conference on CICMT, Baltimore, Maryland, April, 2005
- [3] Currle U.: "Funktionelle Partikeltinten für den Inkjet-Druck von mikroelektronischen Strukturen" (*Functional particle inks for inkjet printing of microelectronic structures*). Dr.-Ing. thesis, Helmut-Schmidt-University, Hamburg, 2010
- [4] Reichl H.: "Hybridintegration", 2. edition, Dr. Alfred Hüthig Verlag, Heidelberg, 1988
- [5] Naghib-Zadeh H. et al.: "BaTiO<sub>3</sub>-based High-k Composition with LTCC Compatible Sintering Temperature". Proceedings 4<sup>th</sup> Internat. Conf. on CICMT, Munich, Germany, April, 2008
- [6] Barth St.: "Entwicklung niedrigsinternder Funktionswerkstoffe für LTCC-Bauelemente" (*Development of low-sintering materials for LTCC elements*). Deutsche IMAPS-Konferenz, Munich, Germany, October, 2008
- [7] Wassmer M.; Diel W.; Krueger K.: "Inkjet Printing of Post-fired Thick-film Capacitors". Proceedings 5<sup>th</sup> Internat. Conference on CICMT, Denver, Colorado, April, 2009
- [8] Diel W. et al.: "Einfluss unterschiedlicher Dielektrika bei der Realisierung von Dickschichtkondensatoren im Tintenstrahl-druck". German IMAPS-Conference, Munich, Germany, October, 2009
- [9] Perrone R.A.: "Erweiterung des Frequenzbereichs und der Integrationsdichte von LTCC-Modulen mittels Photostrukturierung und Designoptimierung". Dr.-Ing. Thesis, TU Ilmenau, 2007

- [10] Muerbe J.; Toepfer J.: "Ni-Cu-Zn Ferrites for Low Temperature Firing: I. Ferrite Composition and its Effect on Sintering Behavior and Permeability". *Journal of Electroceramics*, Vol. 15, pp 215-221, 2005
- [11] Hahn R.; Krumbholz St.; Reichl H.: „Low Profile Power Inductors Based on Ferromagnetic LTCC Technology". *Proceedings Electronic component and technology conference*, pp. 528-533, San Diego, California, May, 2006
- [12] Wassmer M.; Diel W.; Krueger K.: "Inkjet Printing of Fine Line Inductors". *J. Microelectronics and Electronic Packaging*, -in review-
- [13] Hrovat, M. et al.: "Thick-film Strain and Temperature Sensors on LTCC Substrates". *Microelectronics Internat.*, Vol. 23, p.3341, 2006
- [14] Valldorf J.; Gessner W.: "Advanced Microsystems for Automotive Applications 2005". Springer, Berlin Heidelberg, 2005
- [15] Cai Z. et al.: "Fabrication of Microheater by Laser Micro Cladding Electronic Paste". *Materials Science and Engineering*, Vol. 157, pp. 15-19, 2009
- [16] Krüger K.: "Eigenschaften von Mikrohybrid-Dickschichtwiderständen". *PLUS*, Vol. 2, No. 12, pp. 1965-1971, 2000
- [17] Ulrich R.K.; Schaper L.W.: "Integrated Passive Component Technology, 1<sup>st</sup> edition, IEEE Press, Piscataway, 2003
- [18] Barlow F.D.; Elshabini A.: "Ceramic Interconnect Technology Handbook". CRC Press, Boca Raton, 2007
- [19] Birol H.; Maeder T.; Ryser P.: "Influence of Processing and Conduction Materials on Properties of Co-fired Resistors in LTCC structures". *J. European Ceramic Society*, Vol. 26, pp. 1937-1941, 2006
- [20] Pike G.E.; Seager C.H.: "Electrical Properties and Conduction Mechanisms of Ru Based Thick Film (Cermet) Resistors". *J. Applied Physics*, Vol. 48, No. 12, pp. 5152-5169, 1977
- [21] Wang Ch.: "Entwicklung hochohmiger Dickschicht-Widerstandspasten für mikroelektronische Hybridschaltungen". *Dr.-Ing. thesis*, University Erlangen-Nürnberg, 1999
- [22] Abe O.; Taketa Y.: "Mathematical Relation Between RuO<sub>2</sub> Volume Fraction and Resistance of Thick-film Resistors". *J. Applied Physics*, No. 22, pp. 1777-1781, 1989
- [23] Lee J.; Vest R.W.: "Firing Studies with a Model Thick Film Resistor System". *IEEE Transactions on Components, Hybrids and Manufacturing Technology*, Vol. CHMT-6, No. 4, December, pp. 430-435, 1983
- [24] Rodriguez M.A. et al.: "Microstructure and Phase Development of Buried Resistors in Low Temperature Co-fired Ceramic". *J. Electroceramics*, Vol. 5, No. 3, pp. 217-223, 2000
- [25] Cattaneo A. et al.: "Influence of the Substrate on the Electrical Properties of Thick-Film Resistors". *IEEE Transactions on Components, Hybrids and Manufacturing Technology*, Vol. CHMT-3, No. 1, March, pp 181-186, 1980
- [26] Mleczko K. et al.: "Evaluation of Conductive-to-resistive Layers Interaction in Thick-film Resistors". *Microelectronics Reliability*, Vol. 48, pp. 881-885, 2008
- [27] Zheng Y. et al.: "A Study of some Production Parameter Effects on the Resistance-temperature Characteristics of Thick Film Strain Gauges". *J. Physics D: Applied Physics*, Vol. 35, pp. 1282-1289, 2002
- [28] Sutterlin R.C.; Dayton G.O.; Biggers J.V.: "Thick-Film Resistor/Dielectric Interactions in a Low Temperature Co-fired Ceramic Package". *IEEE Transactions on Components, Packaging and Manufacturing Technology*, Vol. 18, No. 2, May, pp. 346-352, 1995